

Fire Location for High and Large-Span Space Buildings based on Binocular Stereo Vision

Lu Ying^{*,1,2}, Wang Huiqin², Wang Ke²

¹*School of Architecture, Xi'an Univ. of Arch & Tech., Xi'an, Shanxi, 710055, P.R. China*

²*School of Information and Control Engineering, Xi'an Univ. of Arch & Tech., Xi'an, Shanxi, 710055, P.R. China*
applepeas@126.com

Abstract

To meet the demand for the early location of fire in large-span space buildings, an accurate fire location method is proposed based on machine vision technology. A nonlinear implicit camera calibration method is proposed by combining an improved particle swarm optimization (PSO) method with least squares support vector machine (LS-SVM) to solve the problem that it is difficult to establish accurate mathematical models for traditional nonlinear explicit camera calibration. The matched pixel coordinates of images collected by cameras are used as input, and the output is the world coordinates. The IPSO is used to search the optimal parameters of LS-SVM regression model to increase the convergence speed and improve the generalization ability of LS-SVM. The spatial location of fire is achieved by three-dimensional reconstruction. The proposed method is applied to fire location for high and large buildings, and experimental results show that the method is effective, fast and accurate.

Keywords: *high and large-span space, camera calibration, fire location, particle swarm optimization (PSO), least squares support vector machine (LS-SVM)*

1. Introduction

With the high-speed development of Chinese economy, there are more and more high and large-span space buildings, such as stadiums, cinemas, shopping malls, *etc.* At the same time of providing people with convenience, these buildings bring challenges to fire safety of them^[1]. Early fire detection and fighting is an effective way of reducing losses of fires. Thus research on early fire detection and automatic location and extinguishing for high and large-span space buildings is very significant. Currently, temperature sensing type, smoke sensing type and compound type fire detectors are mainly adopted in traditional fire detection and extinguishing systems. However due to detecting distance, height or other reasons, these devices can only alarm but fail to locate the fire. With the development of machine vision technology, using surveillance cameras to detect and locate fire becomes feasible and has more advantages^[2-3]. Compared with traditional detection methods, the video surveillance based detection methods are not only fast, but also their monitoring and detection range are wider. Presently, binocular vision systems have been well applied to three-dimensional (3D) measurement and robot vision^[4-6]. However there are few studies on fire source detection based on binocular vision. In this paper, an accurate fire source location method for high and large-span space buildings is proposed based on binocular vision.

Camera calibration is an important topic in computer vision and is an unavoidable problem in stereo vision. The purpose of camera calibration is to establish the mapping relation between two-dimensional (2D) image coordinates and 3D world coordinates. The

imaging process of cameras is affected by many factors, such as optical media, lens distortion, *etc.*, which makes the mapping between 2D image coordinates and 3D world coordinates complex and nonlinear. How to accurately approximate this kind of nonlinear mapping determines the accuracy of camera calibration, and thereby affects the overall measurement accuracy of the vision system. In [7], traditional neural networks (NN) were used to calibrate the stereo cameras. However back propagation (BP) NN is a kind of heuristic method based on experience, and the empirical risk minimization principle is used in training process. Therefore in cases with small sample sets, it is very likely to get over learning and low generalization ability. In [8], an improved genetic algorithm (GA) was used to calibrate stereo cameras. However the performance of GAs will deteriorate when they are used for high dimensional searching, and with the increase of searching space dimension, the performance deterioration is accelerated. In [9], LS-SVM was used to calibrate cameras. The SVM is a kind of new learning method based on statistical learning theory. It is special for small sample sets, and it adopts the structural risk minimization principle. It has strong generalization ability, and overcomes the drawback of NNs, such as over-fitting, slow convergence, easy to get trapped in local minima, *etc.* However, the parameters of SVMs are difficult to choose, which affects their application. In [10], the PSO algorithm was used to search the optimal parameters of LS-SVM, and increased the speed and improved the generalization ability of LS-SVM regression.

In this study, an improved PSO (IPSO) method is used to better adjust the balance between local and global searching ability; then to choose the parameter γ and σ^2 of LS-SVM. Experimental results show that the camera calibration method based on the IPSO and LS-SVM is accurate with fast convergence speed and strong generalization ability, and it is suitable for accurate fire source location for high and large-span space buildings.

2. Basic Theories

2.1 Camera Imaging Model

2.1.1 Monocular Camera Calibration Model: As is shown in Figure 1, $CX_cY_cZ_c$ is the camera coordinate, and $WX_wY_wZ_w$ is the world coordinate. Let the homogeneous coordinates of a point Q in the space in world coordinate be $[x_w, y_w, z_w, 1]^T$. C is the optical center of the camera, and Z_c axis is the optical axis of the camera. O_iXY is the image coordinate of the camera. Image center O_i is the intersection of the optical axis Z_c and image plane of the camera. X and Y axes are parallel to the X_c and Y_c axes of camera coordinate, respectively. Ouv is the image pixel coordinates of the camera. The coordinate unit of the captured images saved in the frame buffers of computers is in the form of pixel numbers. (u, v) is the image coordinates of spatial point Q under the ideal model of pinhole imaging,

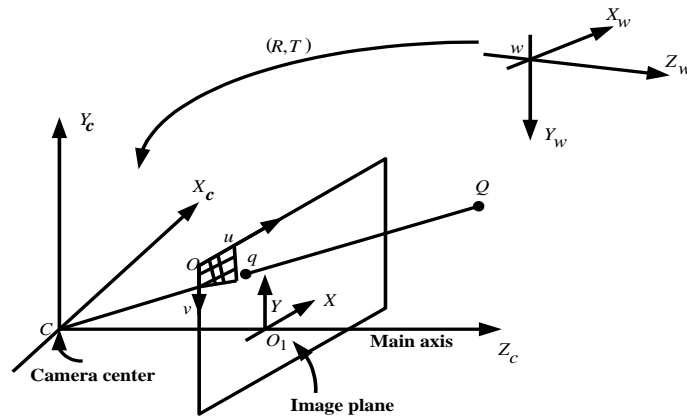


Figure 1. Camera Model

which has the following relation with world coordinate $[x_w, y_w, z_w, 1]^T$:

$$Z_c \begin{bmatrix} u \\ v \\ 1 \end{bmatrix} = \mathbf{M} \begin{bmatrix} x_w \\ y_w \\ z_w \\ 1 \end{bmatrix} = \begin{bmatrix} m_{11} & m_{12} & m_{13} & m_{14} \\ m_{21} & m_{22} & m_{23} & m_{24} \\ m_{31} & m_{32} & m_{33} & m_{34} \end{bmatrix} \begin{bmatrix} x_w \\ y_w \\ z_w \\ 1 \end{bmatrix} \quad (1)$$

2.1.2 Binocular Camera Calibration Model

The two images of the fire source in the space captured by the left and right cameras are shown in Figure 2.

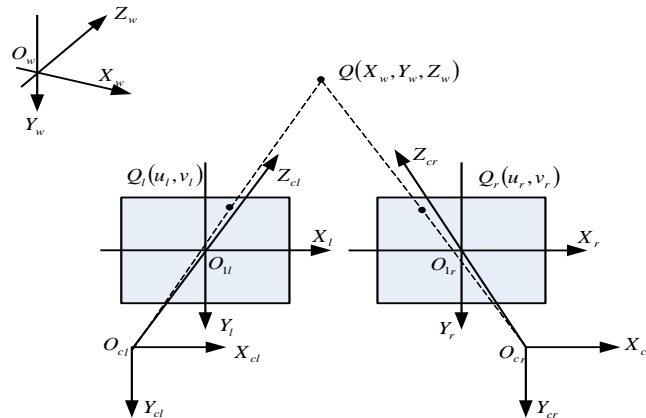


Figure 2. Binocular Stereo Vision Model

The coordinates of the fire source for the two cameras are expressed by (u_l, v_l) and (u_r, v_r) , respectively. The 3D position (x_w, y_w, z_w) is uniquely determined. Assume the projection matrices of the two cameras are M_l and M_r , respectively, which can be obtained by calibration. Then we have:

$$Z_{cl} \begin{bmatrix} u_l \\ v_l \\ 1 \end{bmatrix} = \mathbf{M}_l \begin{bmatrix} x_w \\ y_w \\ z_w \\ 1 \end{bmatrix} = \begin{bmatrix} m_{l11} & m_{l12} & m_{l13} & m_{l14} \\ m_{l21} & m_{l22} & m_{l23} & m_{l24} \\ m_{l31} & m_{l32} & m_{l33} & m_{l34} \end{bmatrix} \begin{bmatrix} x_w \\ y_w \\ z_w \\ 1 \end{bmatrix} \quad (3)$$

$$Z_{cr} \begin{bmatrix} u_r \\ v_r \\ 1 \end{bmatrix} = \mathbf{M}_r \begin{bmatrix} x_w \\ y_w \\ z_w \\ 1 \end{bmatrix} = \begin{bmatrix} m_{r11} & m_{r12} & m_{r13} & m_{r14} \\ m_{r21} & m_{r22} & m_{r23} & m_{r24} \\ m_{r31} & m_{r32} & m_{r33} & m_{r34} \end{bmatrix} \begin{bmatrix} x_w \\ y_w \\ z_w \\ 1 \end{bmatrix} \quad (4)$$

where:

Z_{cl} , Z_{rl} --- scale factors;

$(u_l, v_l, 1)$, $(u_r, v_r, 1)$ --- the image homogeneous coordinates of q_l and q_r in the left and right images, respectively;

$(x_w, y_w, z_w, 1)$ --- the homogeneous coordinates of Q in the world coordinate;

\mathbf{M}_l , \mathbf{M}_r --- the projection matrices of the left and right cameras, respectively.

According to (3) and (4), we can solve the world coordinate of the spatial point Q .

The linear camera model assumes there is no distortion of camera^[11-15]. However, actually, there is more or less distortion of camera lenses. To obtain high accuracy of calibration, a number of nonlinear camera models considering more distortion effects have been proposed^[16-22]. However more nonlinear parameters mean more complicated mathematical models, which complicates camera calibration, and reduces the real-time degree of algorithms. LS-SVM has very strong nonlinear mapping ability, and it can well fit the nonlinear relationship between objects and images. The complex process of solving the parameter or the projection matrix can be avoided by using LS-SVM.

2.2 Improving PSO

The PSO algorithm was initially used to graphically model the elegant yet unpredictable movements of birds^[23,24]. In PSO, a swarm of random particles are initialized, then the optimal solution is obtained by iterations^[25]. In each iteration, particles update themselves by tracking two extrema. The one is the optimum found by the individual particles, which is called individual optimum *pbest*; the other is the optimum found by the whole population, which is the global optimum *gbest*. When the above-mentioned optima are found, particles update their speed and new positions according to the following equation:

$$v_{id}^{k+1} = \omega v_{id}^k + c_1 r_1 (pbest_{id}^k - x_{id}^k) + c_2 r_2 (gbest_{id}^k - x_{id}^k) \quad (5)$$

$$x_{id}^{k+1} = x_{id}^k + v_{id}^{k+1} \quad (6)$$

where:

c_1 , c_2 ---constant acceleration which are in the range of $[0, 4]$, and in general we use

$c_1 = c_2 = 2$;

r_1 , r_2 ---two random variables evenly distributed in $[0, 1]$;

ω --- a non-negative constant, which is called inertia factor.

The position and speed of each particle are initialized randomly. Then the speed of a particle approaches the direction of global optimum and local optimum. ω is a key parameter of PSO, which balances the global and local searching ability of the algorithm. At the initial stage of evolution, we hope the particles have relatively good searching ability. With the increase of iteration number, we hope the particles have relatively good developing ability at the late stage. Therefore the inertia weight should be dynamically adjusted in the evolutionary process, so that particles move in the n -dimensional space at a certain speed. The particles continuously change their speeds and positions under the

effect of themselves and the optimal individual of the population. Finally, the particles fly to the object which is the population center.

The update equation for the speeds and positions of the IPSO:

$$v_{id}^{k+1} = \omega_k v_{id}^k + c_1 r_1 (pbest_{id}^k - x_{id}^k) + c_2 r_2 (gbest_{id}^k - x_{id}^k) + r_3 (pavg_d^k - x_{id}^k) \quad (7)$$

$$\omega_k = (1 - \frac{k}{K_{max}})(\omega_{max} - \omega_{min}) + \omega_{min} \quad (8)$$

$$x_{id}^{k+1} = x_{id}^k + \omega_{k+1} v_{id}^{k+1} \quad (9)$$

Where

v_{id}^{k+1} --- the speed of the i -th particle after the $(k+1)$ -th iteration;

x_{id}^k --- the current position of the i -th particle in the d -th dimension after the k -th iteration;

c_1, c_2 --- acceleration constants, which are normally within $[0,4]$. We use $c_1 = c_2 = 2$;

r_1, r_2, r_3 --- random variables evenly distributed in $[0,1]$;

$pbest_{id}^k$ --- the d -th dimensional component of the optimal position of the i -th particle after the k -th iteration;

$gbest_d^k$ --- the d -th dimensional component of the optimal position of the particle swarm after the k -th iteration;

$\omega_k, \omega_{max},$ and ω_{min} --- the inertia weight, the maximum inertia weight, and the minimum inertia weight of the k -th iteration;

K_{max} --- the largest iteration number.

2.3 LS-SVM Theory

The basic idea of SVM is to map the data of input space to a high-dimensional feature space by a nonlinear mapping, so that a real problem is converted into a quadratic programming problem with an inequality constraint^[26,27]. LS-SVM is the extension of SVM, which replaces the inequality constraint by equality constraint. It uses the squared error loss function as the empirical loss of the training set, thereby converting the real problem into a linear matrix solving problem. The detailed theory is as follows:

Given a sample set $\{x_i, y_i\}_{i=1}^m$, where x_i represents the input vectors and $x_i \in \mathbf{R}^n$; y_i represents the corresponding outputs and $y_i \in \mathbf{R}$. m is the number of the samples. A nonlinear function ϕ maps the samples into a high-dimensional space. Then linear regression is performed with the regression function given by:

$$f(x) = w^T \phi(x) + b \quad (10)$$

where w is the weight vector; b is the bias. The optimization objective function of regression using LS-SVM is:

$$\min J(w, \xi) = \frac{1}{2} w^T w + \frac{1}{2} C \sum_{i=1}^m \xi_i^2$$

$$\text{s.t. } y_i = w\phi(x) + b + \xi_i, i = 1, 2, \dots, m \quad (11)$$

where C is the error penalty function; ξ_i is a relaxation variable. The constructed Lagrange function L is:

$$L(w, b, \xi, a) = \frac{1}{2} w^T w + \frac{1}{2} C \sum_{i=1}^m \xi_i^2 - \sum_{i=1}^m a_i \{w^T \phi(x_i) + b + \xi_i - y_i\} \quad (12)$$

where a_i is the Lagrange multiplier. According to the Karush-Kuhn-Tucker (KKT) conditions, we have:

$$\left\{ \begin{array}{l} \& \frac{\partial L}{\partial w} = 0 \Rightarrow w = \sum_{i=1}^m a_i \phi(x_i) \\ \& \frac{\partial L}{\partial b} = 0 \Rightarrow \sum_{j=1}^m a_j = 0 \\ \& \frac{\partial L}{\partial \xi_i} = 0 \Rightarrow a_i = C \xi_i \\ \& \frac{\partial L}{\partial a_i} = 0 \Rightarrow w^T \phi(x_i) + b + \xi_i - y_i = 0 \end{array} \right. \quad (13)$$

Eliminating w and ξ_i , we have:

$$\begin{bmatrix} 0 & Q^T \\ Q & K + C^{-1}I \end{bmatrix} \begin{bmatrix} b \\ A \end{bmatrix} = \begin{bmatrix} 0 \\ Y \end{bmatrix} \quad (14)$$

where $Q = [1, \dots, 1]^T$; $A = [a_1, a_2, \dots, a_m]^T$; $Y = [y_1, y_2, \dots, y_m]^T$. According to Mercer condition, the kernel function can be determined:

$$K(x_i, x_j) = \phi(x_i)^T \phi(x_j) \quad (15)$$

The LS-SVM function estimation can be obtained:

$$f(x) = \sum_{i=1}^m a_i K(x, x_i) + b \quad (16)$$

In this study, the radial basis function is used as the kernel function:

$$K(x, x_i) = \exp\left\{-\|x - x_i\|^2 / 2\sigma^2\right\} \quad (17)$$

where σ is the width of the kernel function.

From the LS-SVM regression theory, we know that its main parameters include the kernel function parameter σ and the penalty factor C , which have major impact on the learning and generalization ability of LS-SVM. In this study, we use an IPSO algorithm to choose these two parameters, reducing the blindness of empirically choosing them to some extent.

2.4 IPSO for LS-SVM Parameter Optimization

Using IPSO to optimize LS-SVM model parameters can effectively avoid the time consumption and blindness of normal cross validation. The flowchart of the process is shown in Figure 3. The detailed steps are as follows:

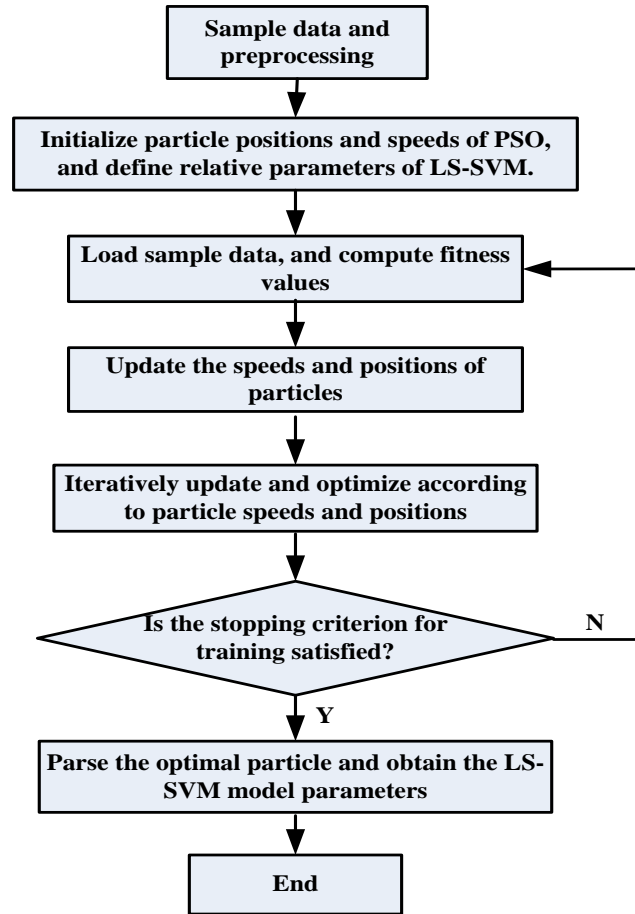


Figure 3. Flow Chart of Optimizing the Parameters of LSSVM based on IPSO

Step1 Initialize the PSO. Set the number of total particles $m = 40$, $D = 2$, $K_{\max} = 800$, $c_1 = 2$, $c_2 = 1.8$, $\omega_{\max} = 0.9$, and $\omega_{\min} = 0.4$. Set the range of γ , σ^2 to $[0, 1000]$ and $[0.001, 10]$, respectively.

Step2 Compute the fitness values of each particle:

$$F(\sigma^2, \gamma) = RMSE \sqrt{\frac{1}{l} \sum_i (y - t)^2} \quad (18)$$

where l is the number of samples; y is the output value of known samples; t is the model prediction value of LS-SVM.

Step3 Update the flying speed and position of the particles; compare the current fitness value of each particle with the fitness value of the particle itself in its optimal position and the fitness value of the population in optimal position. If the current particle is fitter, set the current position of this particle as the optimal position of this particle.

Step4 Check whether the stopping criterion is satisfied. If not, go to **Step5**, and go on computing; if satisfied, compute and output the result.

Step5 $k = k + 1$, go to **Step2**.

Step6 Output $pbest(t)$, and map $pbest(t)$ to the normalized parameters γ and σ^2 .

2.5 LS-SVM Prediction Model based on IPSO

The LS-SVM model based on IPSO is used to predict the internal and external parameters of cameras. The direct calculation of internal and external parameters of

cameras is avoided. The LS-SVM is used as the loss function, which is robust. The calculation speed of the LS-SVM prediction model optimized by the IPSO is significantly increased.

To perform camera calibration, the training of LS-SVM model should be finished at first. The four-input and three-output form is used to realize this kind of mapping relation. As shown in Figure 4, the pixel coordinates (u_l, v_l) , (u_r, v_r) obtained by stereo mapping are used as inputs, and the world coordinate (x_w, y_w, z_w) is the output, so that the given input-output relation is modeled.

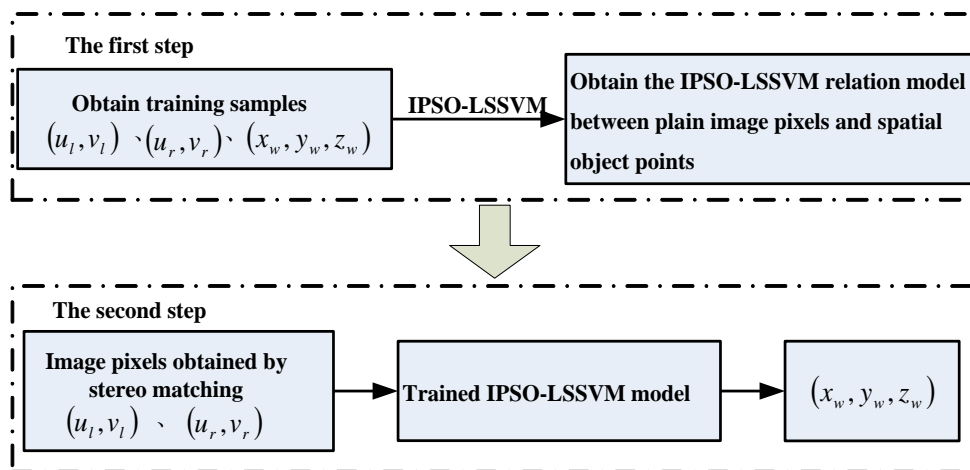


Figure 4. LSSVM Calibration Model

3. Experimental Analysis

3.1 Calibration Experiment

In this experiment, two high-definition network cameras of the same specification are used. The baseline distance is 34 cm. Each black square of the checkerboard is 27×27 mm. There are 6×8 interior angle points in total. Monitoring fire equipments are installed in high places of high and large-span space buildings. Therefore, the origin of the world coordinate is defined as the center of the left and right cameras. Z-axis positive direction is downward parallel to the height direction of calibration board. X-axis positive direction is rightward parallel to the width direction of the calibration board. Y-axis positive direction is backward parallel to the vertical direction of calibration board. Translate the calibration board for 11 positions in the negative direction of Y-axis with each distance between two positions being 30mm. The world coordinate which is closes to the cameras is $y_1 = -30mm$, then $y_{11} = 330mm$. There are 11 positions with each position providing a set of data. A data set of $48 \times 11 = 528$ samples is obtained. Use 458 samples in the data set as training data, and the other 70 are test data. The camera calibration model is shown in Figure 5.

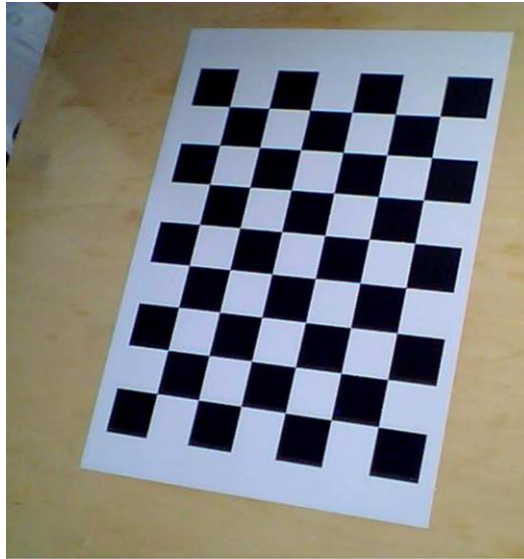


Figure 5. Original Collected Image (Left Camera)

The optimal model parameters for the IPSO-LS-SVM are $\gamma = 51.7$ and $\sigma = 0.34$. Use the LS-SVM calibration model obtained by these two parameters to validate the test samples. A part of calibration results of the test samples as well as the mean square root errors of all points are shown in Table 1. The measurement errors in X, Y, Z directions of camera calibration using BPNN, LS-SVM, PSO-LS-SVM and IPSO-LS-SVM methods are shown in Table 2. It is clear that the calibration accuracy of BPNN and LS-SVM algorithms is relatively low, and the computational complexity of the two algorithms is high. The calibration accuracy of PSO-LSSVM is improved to some extent, and the computational complexity is reduced. The calibration accuracy and the training speed of IPSO-LSSVM method are relatively high.

Table 1. Calibration Results of Partial Test Points

<i>Expect output</i>			<i>IPSO-LSSVM output</i>			e_{mse}
x_w	y_w	z_w	x_w	y_w	z_w	
17	-30	-37	16.932	-30.191	-36.896	0.131
60	-60	-71	60.101	-59.996	-71.359	0.215
100	-90	-52	99.957	-90.129	-52.369	0.227
130	-120	-107	130.523	-120.852	-106.527	0.638
130	-150	-40	130.212	-150.687	-40.514	0.510
70	-180	-87	69.886	-180.265	-86.815	0.198
110	-210	-90	110.135	-209.523	-89.389	0.454
50	-300	-110	50.146	-300.282	-109.727	0.242
90	-330	-110	89.901	-330.058	-110.197	0.132

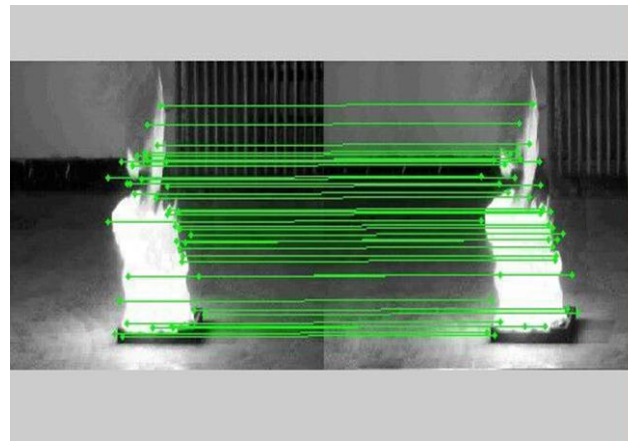
Table 2. Comparison Results of Partial Test Points with Different Methods

<i>Methods</i>	<i>MSE/mm</i>			<i>Time/s</i>
	x_w	y_w	z_w	
<i>BP</i>	0.356	0.812	0.513	13.53
<i>LSSVM</i>	0.269	0.682	0.419	15.27
<i>PSO-LSSVM</i>	0.131	0.412	0.301	6.25
<i>IPSO-LSSVM</i>	0.085	0.312	0.200	3.57

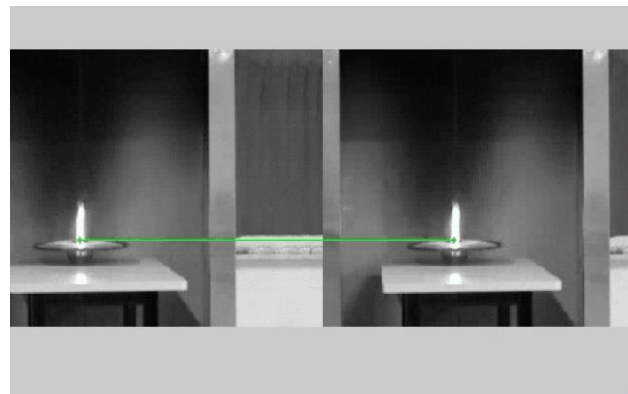
3.2 Calculation of 3D Position of Fire Source

To calculate the position of binocular spatial fire sources, we need the spatial coordinates of fire restored by using the information obtained from the two cameras. Moreover, we need recognize fire in images. The stereo matching of fire images is beyond the scope of this study.

In real applications, the system is composed of two cameras, a calibration board, a burning plate, a fire water cannon and a computer. Choose two test images which are obtained in different spaces to experiment. The fire image matching results are shown in Figure 6.



(a)The first team matching pictures



(b) The second team matching pictures

Figure 6. Matching Results of Flame Pictures

To validate the accuracy of the proposed fire location method, we carry out 8 experiments for each of the traditional Zhengyou Zhang's calibration algorithm and the proposed implicit calibration method under the same matching conditions. The comparison of average error is shown in Table 3. It is clear that the proposed method achieves higher accuracy and the established camera calibration model is more practical. The error in Y-direction is larger than that in X-direction and Z-direction. This error comes from real measurement, because the world coordinate is at the center of the two cameras. The location accuracy of the proposed method is higher than that of Zhengyou Zhang's calibration algorithm, which meet the demand for high and large-span space buildings.

Table 3. Comparison Positioning Results of Flames in High and Large-Span Space Buildings

Group	Error type	Location by Zhengyou Zhang's calibration	Location by the proposed method
The first group of fire	Distance error in X-direction /mm	45	19
	Distance error in Y-direction /mm	76	41
	Distance error in Z-direction /mm	58	26
	Horizontal angle error /($^{\circ}$)	0.25	0.08
	Vertical angle error /($^{\circ}$)	0.32	0.12
The second group of fire	Distance error in X-direction /mm	35	12
	Distance error in Y-direction /mm	48	31
	Distance error in Z-direction /mm	37	22
	Horizontal angle error /($^{\circ}$)	0.19	0.07
	Vertical angle error /($^{\circ}$)	0.21	0.09

5. Conclusions

From the above-mentioned content, an accurate binocular vision location technology in high and large-span space building is proposed. The camera calibration is realized by improving PSO-LSSVM model and the location speed, accuracy and stability are increased. This study can be applied to fire fighting projects of high and large-span space buildings. It takes less than 20s from the fire starts to the fire water cannon finish locating the fire, making unattended fire monitoring and automatic fire location and extinguishing possible. However, there are drawbacks of the proposed method. That is, although the implicit calibration of IPSO-LSSVM is relatively accurate and robust, accurate training samples are difficult to obtain.

Conflict of Interest

The author confirms that this article content has no conflict of interest.

Acknowledgements

This work was financially supported by the Specialized Research Fund for the Doctoral Program of Higher Education (20126120110008), the special scientific research plan project of Shaanxi Province Education Office Foundation(2013JK1144), and the youth fundation of Xi'an University of Architecture and Technology (QN1429).

Finally, Sincere thank teacher Wang the way to my patience careful guidance in the practice of scientific research and paper writing. At the same time, I would also like to thank the members of the research team for their help. The authors are grateful to the anonymous reviewers for their helpful comments and constructive suggestions.

References

- [1] HOU Jie, QIAN Jia-ru, ZHAO Zou-zhou, *et al.*, "Research on Fire Detection and Putting out Technology for High and Large-span Space Buildings" *Journal of Huazhong University of Science and Technology (Urban Science Edition)*, vol. 25, no. 4, pp. 196-202, 2008.
- [2] Ko B C, Cheong K H, Nam J Y, "Fire detection based on vision sensor and support vector machines", *Fire Safety Journal*, vol. 44, no. 3, pp. 322-329, 2009.

- [3] Borges P V K, Izquierdo E, "A probabilistic approach for vision-based fire detection in videos", *IEEE Transactions on Circuits and Systems for Video Technology*, vol. 20, no. 5, pp. 721-731, 2010.
- [4] H. Du, M.G. Li, "The study for particle image velocimetry system based on binocular vision", *Measurement*, vol. 42, no. 4, pp. 619-627, 2009.
- [5] M. Lauer, M. Schönbein, S. Lange, *et al.*, "3D-objecttracking with a mixed omnidirectional stereo camera system", *Mechatronics* vol. 21, no. 2, pp. 390-398, 2011.
- [6] P. Zhao, N.H. Wang, "Precise perimeter measurement for 3D object with a binocular stereo vision measurement system", *Optik* vol. 121, no. 10, pp. 953-957, 2010.
- [7] LÜ Chao-hui, ZHANG Zhao-yang, AN Ping, "Camera Calibration for Stereo Vision Based on Neural Network", *Chinese Journal of Mechanical Engineering*, vol. 39, no. 9, pp. 93-96, 2003.
- [8] ZHANG Ke, XU Bin, TANG Li-xin, *et al.*, "Camera Calibration of Stereo Vision System Based on Genetic Algorithms", *Computer Engineering and Applications*, vol. 42, no. 1, pp. 1-4, 2006.
- [9] LIU Sheng, FU Hui-xuan, WANG Yu-chao, "Camera Calibration for Stereo Vision Based on LS-SVM", *Opto-Electronic Engineering* vol. 35, no. 10, pp. 21-25, 2008.
- [10] LIU Jin-song, YUAN si-cong, JIANG Xiang-kui, *et al.*, "Camera calibration based on PSO and LSSVM regression", *Opto-Electronic Engineering*, vol. 37, no. 5, pp. 47-51, 2010.
- [11] M. Lauer, M. Schonbein, S. Lange, *et al.*, "3D-objecttracking with a mixed omnidirectional stereo camera system", *Mechatronics* vol. 21, no. 5, pp. 390-398, 2011.
- [12] P. Zhao, N.H. Wang, "Precise perimeter measurement for 3D object with a binocular stereo vision measurement system", *Optik*, vol. 121, no. 10, pp.953-957, 2010.
- [13] Z.Z. Xiao, L. Jin, D.H. Yu, *et al.*, "A cross-target-based accurate calibration method of binocular stereo systems with large-scale field-of-view", *Measurement*, vol. 43, no. 6, pp.747-754, 2010.
- [14] Z.P. Cui, G. Jiang, S. Yang, C. Wu, "A new fast motion estimation algorithm based on the loop-epipolar constraint for multiview video coding, Signal Process", *Image Communication*, vol. 27, no. 2, pp.172-179, 2012.
- [15] P.Wang N H, "Precise perimeter measurement for 3D object with a binocular stereo vision measurement system", *Optik-International Journal of Light and Electon Optik*, vol. 121, no. 10, pp.953-957, 2010.
- [16] Blake R, Wilson H, "Binocular vision", *Vision Research*, vol. 15, no. 7, pp.754-770, 2011.
- [17] Eileen E.Birch, "Amblyopia and binocular vision", *Progress in Retinal and Eye Research*, vol. 33, no.3, pp.67-84, 2013.
- [18] Shitai Bao, Ningchuan Xiao, Zehui Lai, Heyuan Zhang, Changjoo Kim, "Optimizing watchtower locations for forest fire monitoring using location models", *Fire Safety Journal*, vol. 71, no.1, pp.100-109, 2015.
- [19] Alan T.Murray, "Optimising the spatial location for urban fire stations", *Fire Safety Journal*, vol. 62, no.11, pp.64-71, 2013.
- [20] Xiaoping Zhou, Hantao Zhang, Lei Sun, "Research on Location Technology in Building Fire Rescue", *AASRI Prodedia*, vol. 3, no.11, pp.445-450, 2012.
- [21] Zhenxing wang, Zhouqi Wu, Xijin Zhen, Rundang Yang, Juntong Xi, "An onsite structure parameters calibration of large FOV binocular stereovision based on small-size 2D target", *Optik-International Journal for Light and Electon Optics*, vol. 124, no.21, pp.5164-5169, 2013.
- [22] T.Song, B.P.Tang, J.M. Xi, "Improvement of the method for space fire positioning based on binocular stereo vision", *J.Chongqing Univ*, vol. 35, no.9, pp.16-21, 2012.
- [23] P.J.García Nieto, J.R.Alonso Fernández, V.M.González, C.Díaz Muñoz, E.García-Gonzalo, R.Mayo Bayón, "A hybrid PSO optimized SVM-based method for predicting of the cyanotoxin content from experimental cyanobacteria concentrations in the Trasona reservoir: A case study in Northern Spain", *Applied Mathematics and Computation*, vol. 260, no.1, pp.170-187, 2015.
- [24] M.Karimi-Nasab, M.Modarres, S.M.Seyedhoseini, "A self-adaptive PSO for joint lot sizing and shop scheduling with compressible process times", *Applied Soft Computing*, vol. 27, no.2, pp.137-147, 2015.
- [25] P.J.García Nieto, E.García-Gonzalo, J.R.Alonso Fernández, C.Díaz Muñoz, "Hybrid PSO-SVM-based method for long-term forecasting of turbidity in the Nalón river basin: A case study in Northern Spain", *Ecological Engineering*, vol. 73, no.12, pp.192-200, 2014.
- [26] C.Rajeswari, B.Sathiyabhama, S.Devendiran, K.Manivannan, "Bearing Fault Diagnosis using Wavelet Packet Transform, Hybrid PSO and Support Vector Machine", *Procedia Engineering*, vol. 97, no.12, pp.1772-1783, 2014.
- [27] Abdulhamit Subasi, "Classification of EMG signals using PSO optimized SVM for diagnosis of neuromuscular disorders", *Computers in Biology and Medicine*, vol. 43, no.5, pp.576-586, 2013.